ISSN:2790-1688 Volume-15-(2025)

Numerical Investigation of an Embedded-Configuration Evaporating Tube-Type Combustor

Jiayong Chen [1, *], Yubing Lei [1]

[1]College of Energy and Engineering, Nanjing University of Aeronautics and Astronautics, China.

Abstract. To address the trend of the axial position of the inlet diffuser outlet extending downstream in micro/small aero-engine combustors, an embedded combustor layout is proposed, featuring the combustor liner head positioned forward within the cavity adjacent to the diffuser hub side, thereby effectively shortening the combustor length. Hot-state three-dimensional simulations were performed on this layout based on a specific MTF engine model. Its vortex structure and combustion organization characteristics were analyzed using the flow field, fuel spray field, temperature field, outlet temperature distribution, and wall temperature profiles. These findings provide a theoretical basis for the optimal design of this embedded combustor configuration.

Keywords: Evaporating tube-type annular combustor; Micro combustor; numerical simulation.

1. Introduction

The combustors primarily utilized in new-generation micro engines are classified into two main types: throughflow annular combustors and recirculation annular combustors. For micro turbojet engines (MTEs) in the thrust class of 100N, the evaporating tube fuel supply system is generally employed[1]. A schematic diagram of a typical evaporating tube-type micro combustor is shown in Fig. 1.

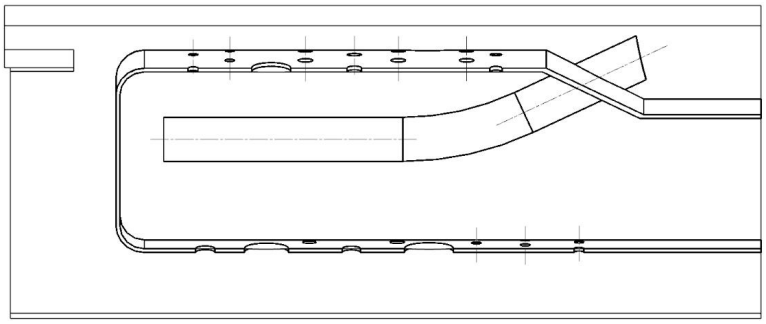

Fig. 1. a typical micro throughflow combustor with rearward evaporating tubes

Guo et al. [2] conducted a numerical simulation study on the evaporating tube-type combustor of a micro turbojet engine with a thrust of 40daN, analyzing performance characteristics such as the combustor's airflow distribution, fuel atomization, and temperature profile. Li Chao et al. [3] investigated the atomization and evaporation performance of both forward and rearward evaporating tubes through experimental and numerical methods. Their results demonstrated that the rearward evaporating tube exhibited a lower pressure loss, and they established a correlation between the main aerodynamic parameters inside the tube and the evaporation efficiency. Li Dongjie et al. [4] analyzed and validated the airflow and combustion processes within the evaporating tube-type micro combustor by comparing simulation and experimental results. Based on their proposed "vortex-entrained liquid" design concept, they optimized the combustor’s outlet temperature distribution factor (OTDF) and combustion efficiency. Furthermore, An Yanzhao et al. utilized the Ω vortex evaluation method to conduct an in-depth analysis of the influence of vortex structure and intensity within the primary zone of the evaporating tube-type micro combustor on the mixing and combustion process.

The aforementioned combustors all represent the conventional layout of rearward evaporating tube-type micro throughflow combustors. With the continuous performance improvement of the

upstream component, the compressor, the axial position of the diffuser exit (or compressor outlet) also extends rearward. In previous designs of evaporating tube-type micro combustors, the ratio of the penetration depth of the diffuser hub to the combustor height was typically below 0.2, resulting in insufficient space beneath the hub. However, with the further advancement of compressor technology, this ratio has now significantly exceeded 0.2.

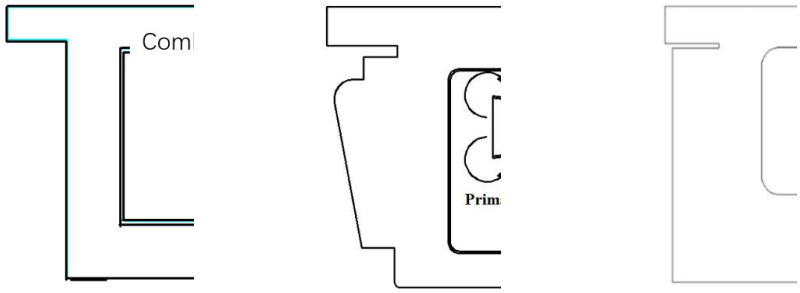

(a) (b) (c)

Fig. 2. The diffuser exit hub extending into the combustor domain

This paper proposes an embedded evaporating tube-type micro throughflow combustor layout, where the combustor liner head is positioned forward within the cavity adjacent to the diffuser hub side, fully utilizing the space beneath the diffuser hub. This layout is applied to a specific model of a micro turbofan engine (MTF), and hot-state three-dimensional simulations are performed using Fluent software. Furthermore, its vortex structure and combustion organization characteristics are analyzed based on the flow field, fuel spray field, temperature field, outlet temperature distribution, and wall temperature profiles.

2. Simulation setup

2.1 Combustor model and Grid generation

The combustor of a certain micro turbofan engine is a rearward evaporating tube-type micro annular throughflow combustor, and its modified embedded layout structure is shown in the Fig. 3. Due to the inherent periodic symmetry within the micro combustor, and to minimize computational effort, a one-twelfth sector of the full annulus (i.e., an angular periodicity of 30°) is selected for modeling, meshing, and calculation based on the number of evaporating tubes. This approach is sufficient to completely simulate the internal flow and combustion characteristics of the micro combustor.

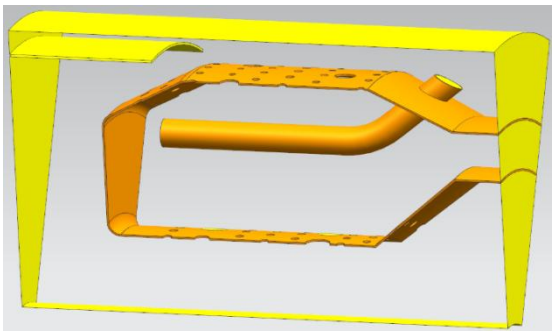

Fig. 3. Geometric Configuration

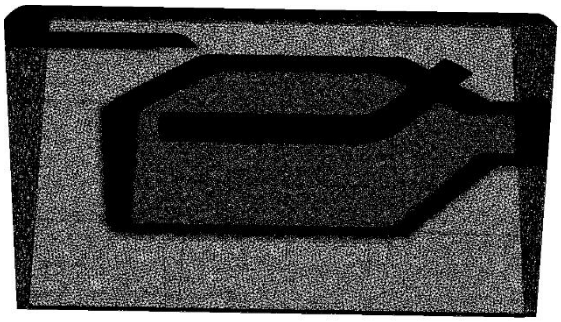

Fig. 4. Grid Generation

The combustor was meshed using non-structural grids (or unstructured mesh) generated by the ICEM software. Grid refinement was applied to the interior of the combustor liner and the evaporating tube regions. The meshing model is illustrated in Fig. 4.

The number of grids impacts the computational speed and cost. Grid independence verification was conducted in Section 2.3 for models with 4.52 million, 5.74 million, 6.96 million, 8.03 million, and 9.47 million elements.

2.2 Boundary set up.

Due to the complex vortex structure within the combustor, the Fluent software was selected as the solver. The turbulence model chosen was the k-epsilon two-equation model. The motion and evaporation of oil droplets inside the evaporating tube were simulated using the Discrete Phase Model (DPM), specifically its three-term model. The species transport model, considering both kinetic and turbulent factors, adopted the Finite Rate/Eddy-Dissipation Model. Second-order upwind schemes were used for the discretization of momentum, species, and energy equations, while the Coupled algorithm was employed for velocity-pressure coupling.

The combustor inlet utilized a mass flow inlet boundary condition, where the air mass flow rate per sector, inlet temperature, pressure, as well as the inlet airflow's turbulence intensity and hydraulic diameter, were specified. The fuel inlet was defined by the coordinates, velocity components, and mass flow rate at the injection point. The droplet particle diameter in the discrete phase adopted the Rosin-Rammler (R-R) distribution. The periodic boundaries were set as a rotational periodic boundary type with a zero-pressure gradient. The combustor outlet was specified as a free outflow with a constant pressure gradient.

2.3 Numerical Method Validation.

Grid independence verification was performed on models with 4.52 million, 5.74 million, 6.96 million, 8.03 million, and 9.47 million elements, using the total pressure recovery coefficient as the validation criterion. The results of the independence verification are presented in Table 1. Selecting the 6.96 million grid count ensured both the required accuracy and a balanced computational cost.

Table1. Grid independent test

Number of grids	4520749	5739521	6961943	8030313	9479522
σ(%)	96.66	96.59	96.42	96.46	96.37

The reliability of the numerical method was validated by comparing the simulation results with the previous experimental data for a certain MTF combustor model. The comparative results are presented in Table 2. Since the relative error is within 1%, the numerical method is confirmed to be reliable.

Table 2. Numerical Method Validation

	T_{t4}(K)	η_b(%)
CFD	902.7	88.9
Experiement	908.2	89.8

3. Result and discussion

The numerically calculated total pressure recovery coefficient and combustion efficiency, compared with the pre-modification scheme, are presented in Table 3. As shown in the table, the combustor adopting the embedded layout exhibits a 0.4% decrease in combustion efficiency and a 1.2% decrease in total pressure recovery coefficient. However, its axial length is reduced to 0.87 times the original length.

Table3. Numerical Results Comparison

	σ(%)	η_b(%)	Relative Combustor Length
Embedded layout	96.38	98.0	0.87

Conventional Layout	97.60	98.4	1.00

Fig. 5 presents the velocity streamline contours. The Angular-0 plane is located exactly at the central axis of the evaporating tube, while the Angular-15 plane is situated in the mid-section between two adjacent evaporating tubes.

The fundamental flow structure of the combustor involves air entering from the inlet. A portion of this airflow flows through the outer annulus, passing through the openings on the outer liner wall and the evaporating tube, before entering the combustor liner. Another portion of the airflow deflects significantly, bypassing the combustor liner head to enter the inner annulus, and then flows into the liner through the openings on the inner liner wall. After converging inside the combustor liner, the airflow exits the combustor axially. The combustor flow resistance is increased due to the obstruction imposed by the combustor liner head on the airflow directed toward the inner annulus, which leads to a reduction in the combustor total pressure recovery coefficient.

At the combustor liner head, the airflow exiting the evaporating tube impacts the front wall of the liner. This impingement causes a loss of kinetic energy, resulting in a reduction of the axial velocity of the post-impingement flow. On the side of the liner head where the radial height is less than the evaporating tube axis (the inner side), the air injected through the primary holes also impinges on the axially moving flow. The mainstream flow is truncated by the primary jet, leading to a noticeable recirculation and the formation of a large-scale vortex. On the side of the liner head where the radial height is greater than the evaporating tube axis (the outer side), due to the proximity of the outer wall to the evaporating tube axis, the small holes on the outer liner head truncate the mainstream flow. This results in the formation of multiple, relatively small-scale vortices between the front face and the outer primary holes. The velocity within these vortex regions is very low, which contributes to flame stabilization and thus favors combustion.

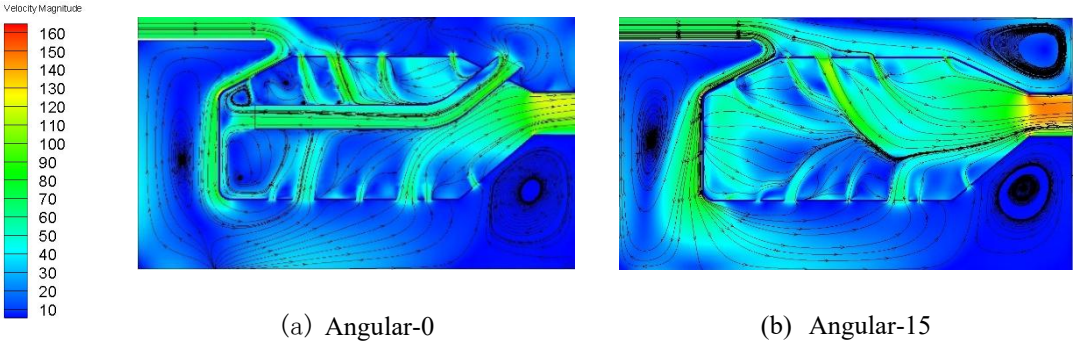

(a) Angular-0 (b) Angular-15

Fig. 5 Velocity streamline contours

Six cross-sections, perpendicular to the axis, were extracted axially within the primary zone to observe and analyze the axial development of the vortex structure in this region. Sections 1 and 2 are located upstream of the evaporating tube exit plane, while the remaining sections are situated downstream. Notably, Sections 5 and 6 pass through the inner and outer primary holes, respectively.

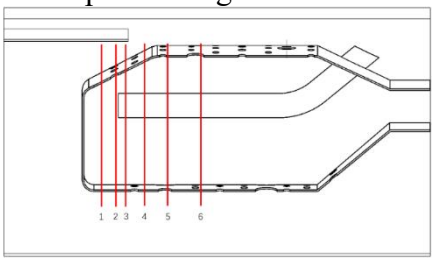

Fig. 6 Illustration of Primary Zone Planes

As observed from the velocity streamline contours of Sections 1 and 2 (Fig. 7(a) and (b)), the airflow exiting the evaporating tube exhibits a circumferential swirl due to the secondary flow within the tube. This circumferential swirl weakens before impinging upon the combustor liner

front face, and diffuses relatively uniformly outward after impact. The airflow between adjacent evaporating tubes is mutually compressed and constrained by the inner wall of the combustor liner, resulting in the formation of two large vortices below the evaporating tube exit.

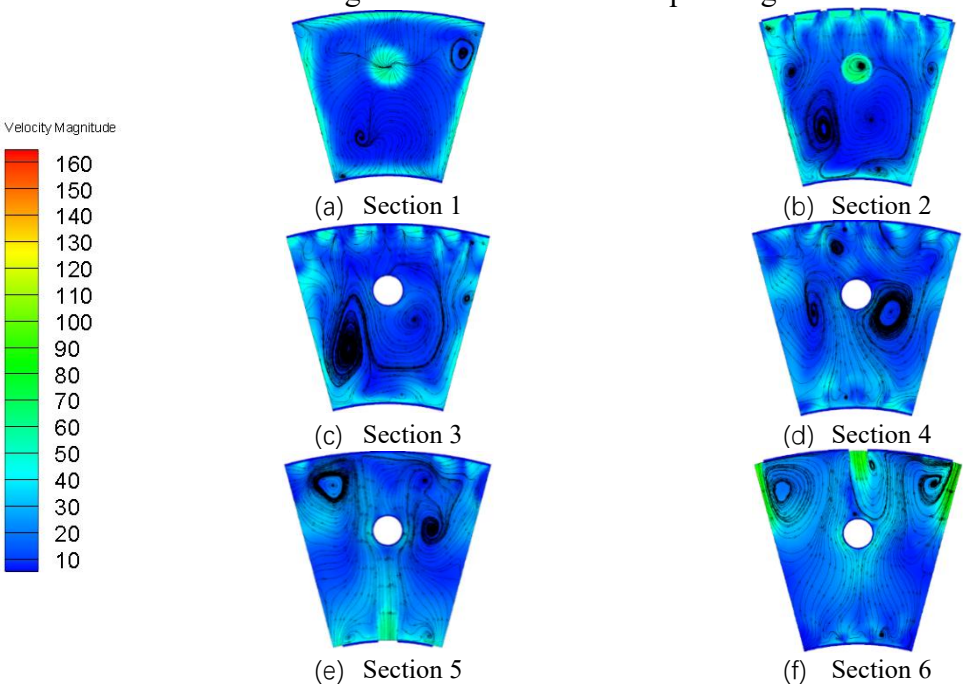

Fig. 7 Velocity Streamline Contours of Primary Zone Cross-Sections

As shown in the velocity streamline contours of Sections 3 and 4 (Fig. 7(c) and (d)), the two large vortices formed upstream continue to develop axially. Influenced by the radial kinetic energy of the inner primary hole jet, these two large vortices gradually migrate towards the outer annulus. Upon further development to the axial location of the outer primary holes, the two large vortices eventually reach the vicinity of the outer wall, where the outer primary hole jet flows into the vortices, as illustrated in Fig. 6(e) and (f).

Overall, the primary zone of the embedded combustor layout features stably developing large vortices. These large vortices facilitate adequate mixing with the primary hole jets, and the rich vortex structure satisfies the basic requirements for fuel-air mixing and flame stabilization in the primary zone. However, in the region of the evaporating tube exit, the vortex flow is predominantly close to the inner wall. The absence of a vortex above the evaporating tube exit leads to poor fuel-air mixing in that section, resulting in fuel droplet aggregation, lower temperature, and difficult combustion, causing the high-temperature zone above the evaporating tube to shift downstream. This observation is consistent with the temperature contours presented later.

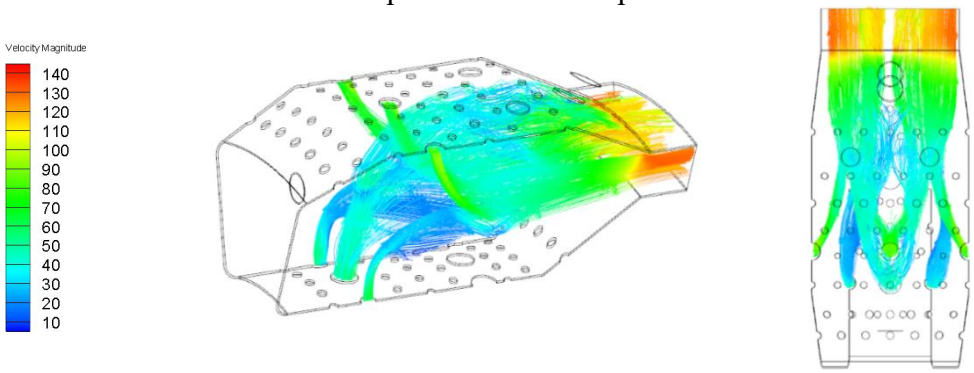

Fig. 8 Primary Hole Jet Streamline Contours

Fig. 8 and Fig. 9 present the primary hole jet streamlines and the primary hole axial cross-section velocity vector diagrams, respectively. Both the inner and outer primary holes are directly opposite

the evaporating tube, creating a head-on jet impingement. This arrangement not only provides effective cooling for the evaporating tube, but the two impinging airflows also cause deceleration upon impact with the tube. Furthermore, the interaction between the decelerated airflows forms two larger vortices in the circumferential direction of the evaporating tube, which is beneficial for increasing gas residence time. Observation of the temperature contours also confirms that the combustion reaction occurs within this low-velocity recirculation zone.

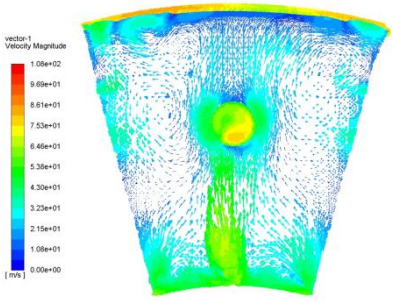

Fig. 9 Velocity Vector Diagram of the Primary Hole Cross-Section

A reasonable fuel spray distribution is essential for ensuring stable and highly efficient combustion. Fig. 10 presents the fuel spray distribution contour of the combustor. The fuel-air mixture is concentrated at the combustor liner head and is distributed relatively uniformly on both the upper and lower sides of the evaporating tube, with the mass fraction of fuel species generally maintained around 0.06. However, due to the constraint imposed by the outer wall of the combustor liner head, fuel droplets accumulate above the evaporating tube.

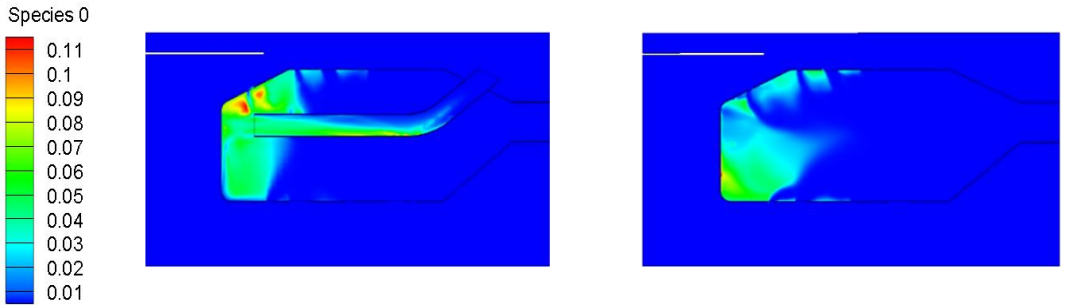

(a)Angular-0 (b)Angular-15

Fig. 10 Fuel Spray Distribution Contour

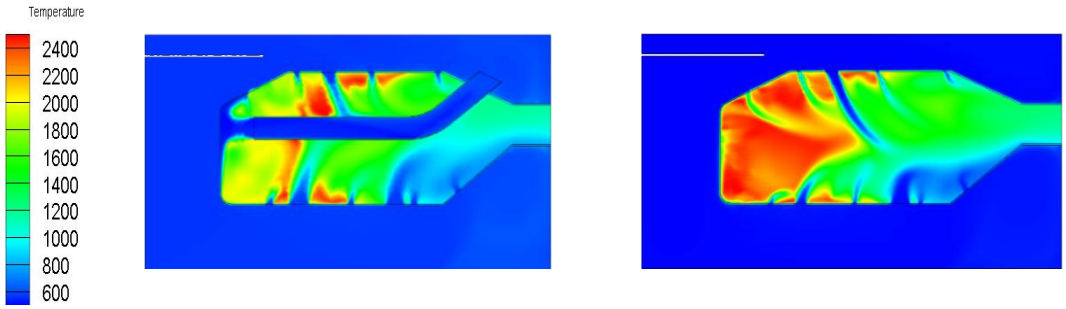

(a)Angular-0 (b)Angular-15

Fig. 11 Temperature Distribution Contour

Fig. 11 shows the temperature distribution contour. It can be seen that, corresponding to the fuel spray distribution, the high-temperature zone above the evaporating tube is relatively rearward in the Angular-0 plane due to the influence of fuel accumulation. In the Angular-15 plane, the high-temperature zone is concentrated within the primary zone of the combustor liner.

A recirculation zone exists at the evaporating tube exit, where fresh fuel-air mixture continuously accumulates and participates in the reaction. Upon entering the combustor liner, the primary hole jet effectively truncates the high-temperature gas and mixes and combusts with the

fully combusted upstream combustible gases near the flame front. Consequently, intense combustion reactions occur within the primary zone.

The Outlet Temperature Distribution Factor (OTDF) is defined as the ratio of the difference between the maximum and average total gas temperature at the combustor exit plane to the actual temperature rise across the combustor. The calculation formula for OTDF is given by Equation (1), Where T_l, T_{t3}, T_{t4}, T_{t4max}represent the maximum total gas temperature at the combustor exit, the average total gas temperature at the combustor exit, and the total temperature at the combustor inlet, respectively.

$$OTDF = \frac{T_{t4max} - T_{t4}}{T_{t4} - T_{t3}} \quad (1)$$

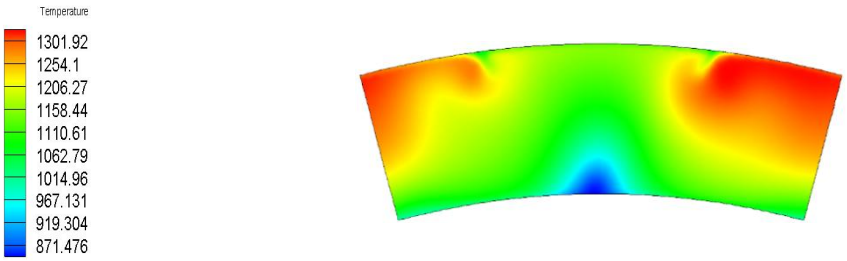

Fig. 12 Outlet Temperature Distribution Contour

Fig. 12 illustrates the total temperature distribution at the combustor exit plane. The average total exit temperature is 1145.88K, and the maximum total exit temperature is 1331.72K. Given that the theoretical temperature rise under design conditions is 632.69K, and the average total inlet temperature is 526.458K, substituting these values into Equation (1) yields an Outlet Temperature Distribution Factor (OTDF) of 0.3 for this scheme.

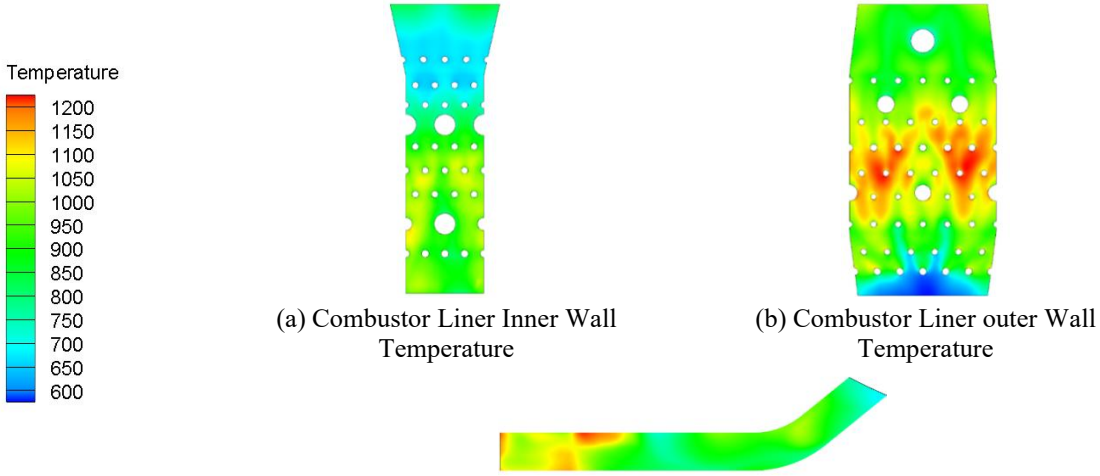

(a) Combustor Liner Inner Wall Temperature

(b) Combustor Liner outer Wall Temperature

(c) evaporating tube Wall Temperature

Fig. 13 Wall Temperature Distribution Contours of the Combustor Liner and Evaporating Tube

Observation of the exit temperature distribution reveals that the high-temperature zone is primarily concentrated near the outer annulus of the combustor liner, specifically distributed on both sides of the evaporating tube. A distinct low-temperature zone appears near the inner annulus, and the total temperature gradually decreases in the direction of decreasing radius. The presence of distinct high-temperature zones on the two sides above the exit is attributed to the vortex structure in the combustor head. As indicated by the preceding vortex structure analysis, two large vortices exist in the upper part of the combustor liner cavity towards the end of the primary zone. These vortices carry uncombusted fuel droplets from upstream, which then mix and combust with the primary hole jet. The lagging of the high-temperature zone results in non-uniform cooling as the

airflow passes through the mixing zone, ultimately leading to the appearance of two distinct hot spots at the exit.

Fig. 13 displays the temperatures of the combustor liner outer wall, the combustor liner inner wall, and the evaporating tube wall. The high-temperature zone on the combustor liner outer wall is concentrated near the primary holes, with a hot spot temperature of 1289.43K. This hot spot distribution corresponds to the internal temperature distribution within the combustor liner. The hot spot temperature of the evaporating tube wall is 1247.01K. In comparison, the temperatures of the combustor liner front face and the combustor liner inner wall are generally lower.

4. Summary

Addressing the developmental trend where the axial position of the inlet diffuser outlet extends downstream in existing micro/small aero-engine combustors, this paper proposes an embedded combustor layout with the combustor liner head positioned forward within the cavity adjacent to the diffuser hub side. This configuration, applied to a specific MTF combustor model, achieves a 13% reduction in combustor length compared to the original design. Hot-state three-dimensional simulations were performed using Fluent software to analyze its vortex structure and combustion organization characteristics.

Results indicate that the new layout compels a portion of the airflow exiting the diffuser to bypass the combustor liner head to enter the inner annulus, which increases the combustor's flow resistance and leads to a 1.2% decrease in the total pressure recovery coefficient. However, the presence of large vortices on both sides of the evaporating tube in the liner head flow field, which develop stably downstream axially and migrate radially towards the outer annulus, allows the combustor to still organize combustion effectively, keeping the combustion efficiency essentially unchanged. Conversely, the absence of a large vortex above the evaporating tube exit results in non-uniform fuel-air mixing in that region. Subsequent mixing and combustion occur downstream, causing the high-temperature zone to migrate downstream, which impacts the wall temperature distribution and the quality of the exit temperature distribution.

References

[1] Li Y Z, Liu J, Xu Q H, et al. Study on vaporization rate of a mini Γ-vaporizer under atmospheric pressure condition. Journal of Aerospace Power, 2006, 21(5): 843 847. (in Chinese)

[2] Guo Y, Jiang X H, Zheng Y. Numerical simulation for the combustor with vaporizing tube of micro turbine engine. Tactical Missile Technology, 2011(1): 109 113. (in Chinese)

[3] Dongjie L, Bohao Z, Qian L, et al. Optimization of a micro turbojet engine combustion chamber. J Tsinghua Univ 2021; 61: 1212–20.

[4] Yanzhao An, Yuzhang Wang, et al. Understanding interaction between flow field vortex and combustion of an evaporating tube-type annular combustor. Feul, 2026: 404(1): 136270

[5] Huang, W. Effect of bleeding air for aircraft auxiliary power unit on combustor flow characteristics. In APISAT 2019: Asia Pacific International Symposium on Aerospace Technology. Engineers Australia.2019:2420-2429.

[6] Mohammad B, Andac M G. Influence of the pri-mary jets and fuel injection on the aerodynamics of a proto-type annular gas turbine combustor sector[J].Journal of Engineering for Gas Turbines and Power, 2011,133 (1): 011505. 1-011505. 8.